DOI: 10.1002/ejic.200500661

Theoretical Study of the Effects of Phosphane Substituents on the Bonding Properties of Acetylene with $Ni(PR_3)_2$ (R = H, CH_3, F, CF_3, C_6H_5)

Manuel Piacenza,[a] Julia Rakow,[a] Isabella Hyla-Kryspin,*[a] and Stefan Grimme*[a]

Keywords: Alkyne ligands / Density functional calculations / Nickel / Phosphane ligands

The bond-formation processes between the d^{10} metal fragments $Ni(PR_3)_2$ (R = H, CH_3, F, CF_3, Ph) and acetylene have been studied by density functional theory with the BP86 functional and large TZV(2df,2pd) basis sets. The Ni–acetylene bonds have been analyzed in terms of distortion and intrinsic interaction energies within the Dewar–Chatt–Duncanson model of bonding. The intrinsic interaction energies have been corrected for basis set superposition error (BSSE). Linear relationships have been found between the intrinsic interaction energies and the distances of the Ni–C and C≡C bonds as well as with the acetylene–nickel π-backbonding. No linear relationship with respect to the total interaction energies was found. Despite using large basis sets, BSSE still contaminates the interaction energies by 5–10 %. For the PR_3 ligands, the BSSE-corrected intrinsic interaction energies of acetylene bonding increase in the order $P(CF_3)_3 < PF_3 < PPh_3 < PH_3 < P(CH_3)_3$ from 58.9 to 77.9 kcal mol^{-1}, while the total interaction energies range from 32.9 to 42.4 kcal mol^{-1} in the order $PPh_3 < P(CF_3)_3 < P(CH_3)_3 < PH_3 < PF_3$. These results reveal that the total influence of PH_3 and PPh_3 on the thermodynamics of the acetylene bonding is different and therefore in this sense PH_3 is not a good model of PPh_3 in theoretical calculations.

Introduction

Alkynes and tertiary phosphanes coordinated to transition metals (TM) have been the subject of extensive experimental and theoretical studies.[1,2] This can be attributed to the specific reactivities of these species, which in the field of organometallic synthesis and catalysis give rise to a wide variety of products.[3,4] Because of the early work of Reppe et al.,[5] it is well known that nickel complexes promote the reactivity of the acetylene triple bond in several catalytic processes such as carbonylation, cyclooligomerization, and cooligomerization. Common to these processes is the presence of acetylene complexes with low-valent $Ni(PR_3)_2$ fragments, where R is mostly a bulky alkyl or aryl group.[3i,6]

In general, the reactivities of coordinated ligands are discussed in terms of steric and electronic effects, although the distinction between them is not always straightforward because both effects are interconnected. The steric properties of PR_3 ligands are usually measured by the cone angle, θ, introduced by Tolman.[7] The steric effects for acetylene are less important, but in the case of alkynes with bulky substituents they may also influence the bonding.[8] The electronic effects of alkynes and phosphanes are inherently connected with the Dewar–Chatt–Duncanson (DCD) model,[9] i.e., with the ability of ligands to act as electron density donors and acceptors. Thus, the electronic contribution to a TM–P bond stems from two factors: a σ-donation from the phosphorus lone-pair orbital to empty metal orbitals, and a π-back-donation from occupied metal orbitals to the virtual σ* P–R MOs of the PR_3 ligands.[10] It is clear that electron-withdrawing substituents change the basicity of the PR_3 ligands and consequently their ability for σ-donation. The classification of donor/acceptor properties of PR_3 ligands has long been of interest in both experimental[7,10b,10c,11] and theoretical studies.[2f,2h,12] Due to the presence of a double π-system in alkyne ligands, two donor and two acceptor interactions are possible. As a result, alkynes exhibit a remarkable flexibility of coordination modes, and are able to act as two- or four-electron donors and to occupy up to four coordination sites.[13,14]

In the present work we are interested in the structural, electronic, and energetic properties of the bond-formation processes shown in Scheme 1.

The chosen phosphane substituents offer a broad variety of steric and electronic effects. While theoretical investigations of the effects of phosphane substituents on direct $TM–PR_3$ bonds are more common,[2f,h,12] investigations of the inductive effects on bonding of other ligands are scarce.[2l] To the best of our knowledge, a systematic study of the inductive effect of phosphane substituents on acetylene bonding in complexes **c**, including electron withdrawing and sterically demanding substituents, has not been reported so far. Furthermore, our chosen substituents should provide insight into the question of whether the PH_3

[a] Organisch-Chemisches Institut der Universität Münster, Corrensstr. 40, 48149 Münster, Germany
E-mail: ihk@uni-muenster.de
grimmes@uni-muenster.de

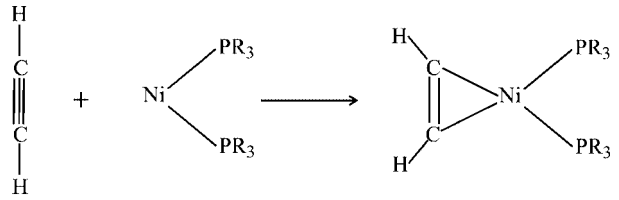

a **b** **c**

R = H (**1**), CH_3 (**2**), CF_3 (**4**), C_6H_5 (**5**)

Scheme 1.

ligand, which is frequently used in theoretical studies as a model for bulky organophosphanes,[2,4a,15] is a good substitute for the PPh_3 ligand, which is more common in experimental studies.

Results and Discussion

Before we discuss our results in more detail, we present a simplified picture (Figure 1) of the well known DCD model for the donor–acceptor interactions between the valence π-MOs of acetylene (**a**) and the metal fragments $Ni(PR_3)_2$ (**b**).

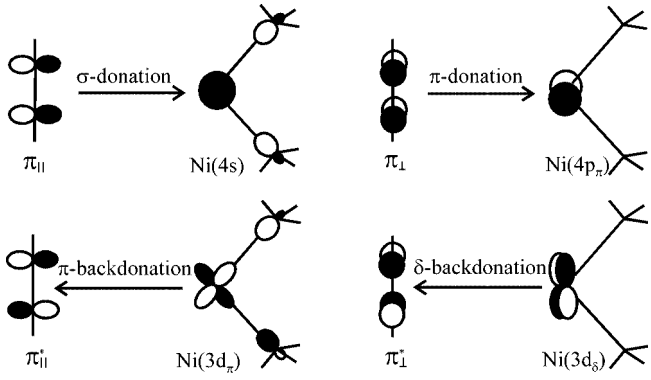

Figure 1. Simplified representation of the DCD model for synergic donor–acceptor interactions between valence MOs of acetylene and $Ni(PR_3)_2$.

Since the nickel 3d levels are fully occupied in complexes **b**, the donation of electron density from acetylene in-plane ($\pi_\parallel$) and out-of-plane ($\pi_\perp$) MOs can take place to the empty nickel levels with predominant 4s and 4p character (Figure 1 top). In these L → TM donation interactions the occupied nickel 3d levels can participate due to second-order mixing only, i.e., due to three-orbital two-electron interactions.[16] In complexes **c** two occupied Ni 3d levels may be involved in backbonding interactions with the empty $\pi_\parallel$* and $\pi_\perp$* MOs of acetylene (Figure 1 bottom). From previous investigations it is well known that the contributions from the out-of-plane L → TM π-donation and M →L δ-back-donation are by far less important than those from the in-plane σ-donation and π-back-donation interactions.[2]

Contrary to homoleptic acetylene–nickel compounds,[13d–13f] complexes **c** prefer a planar molecular structure over a twisted one (Scheme 2).[6,8] In structure **c** the acetylene, nickel, and phosphorus atoms are placed in the same plane while in the twisted structure **c′** the acetylene is rotated by 90° around the C_2 axis. Previous calculations on the model complex **1c** have shown that backbonding interactions from the nickel $3d_\pi$ orbital to the acetylene in-plane $\pi_\parallel$* MO account for the stability and preferred molecular geometry of this class of compounds.[2a–2e,2i,2k] In the planar geometry **c** the acetylene–nickel in-plane π-backbonding interaction is enforced by electron density donation from a phosphorus lone-pair out-of-phase combination, which in the twisted geometry **c′** is not possible (Scheme 2).

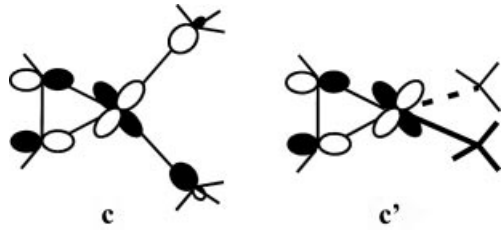

c **c'**

Scheme 2.

In order to find out the preferred arrangements of the phosphane ligands in the planar molecular structure of the acetylene complexes **1c**–**5c** and their molecular fragments **1b**–**5b** we first investigated the rotation of the PR_3 ligands around the Ni–P bond. For **1b**–**4b** and **1c**–**4c** we considered one C_s-symmetric and two C_{2v}-symmetric rotamers (Scheme 3). Complexes **5b** and **5c** were optimized in C_s and C_1 symmetry. For the sake of clarity the lowest energy structures of **5b** and **5c** are shown in Figure 2; the relative energies of the optimized conformers are presented in Table 1 and selected optimized parameters of the lowest energy structures are collected in Table 2. The energetics for the bond formation between acetylene (**a**) and $Ni(PR_3)_2$ (**b**) are summarized in Table 3 and the results of NBO population analyses in Tables 4 and 5.

From Table 1 it is evident that the different rotamers of **1b**–**4b** and **1c**–**4c** are energetically almost equivalent and the lowest energy structures adopt C_{2v} symmetry. For **1b**–**4b**, **1c**, and **3c** the energy differences are below 0.3 kcal mol^{-1} and for **2c** and **4c** they are only slightly larger [0.7 kcal mol^{-1} (**2c**), 0.9 kcal mol^{-1} (**4c**)]. Due to the steric requirements of the PPh_3 ligands, **5b** and **5c** prefer nonsymmetric over C_s-symmetric structures, which are less stable by 9.5 and 2.2 kcal mol^{-1}, respectively (Table 1).

From Table 1 it is also evident that the lowest energy rotamers of the complexes **2c**–**5c** and the metal fragments **2b**–**5b** are characterized by the same conformation of the phosphane ligands. Although the preferred conformation of the phosphane ligands in the metal fragment **1b-2** differs from that in the complex **1c-1**, the energy difference between **1b-1** and **1b-2** (0.1 kcal mol^{-1}) is not relevant for our discussion.

The experimental molecular structures of **1c**–**4c** are not known and only that of **5c** has been determined by X-ray

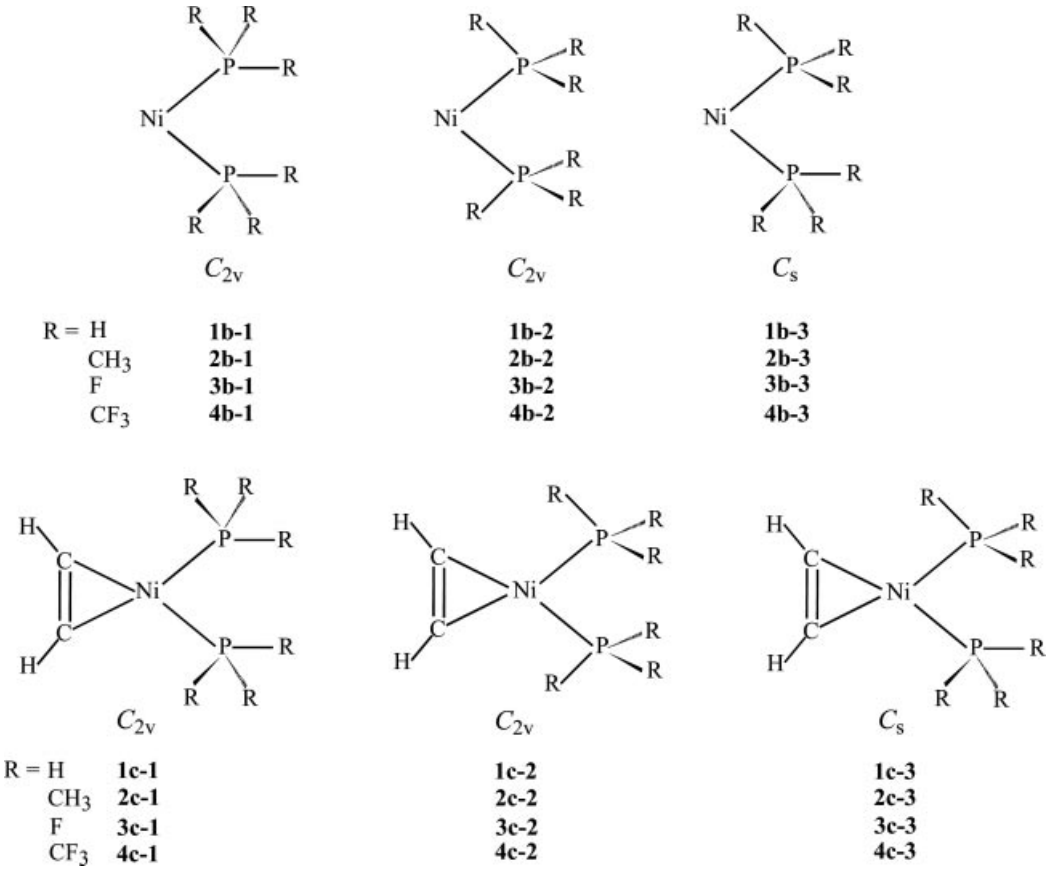

Scheme 3.

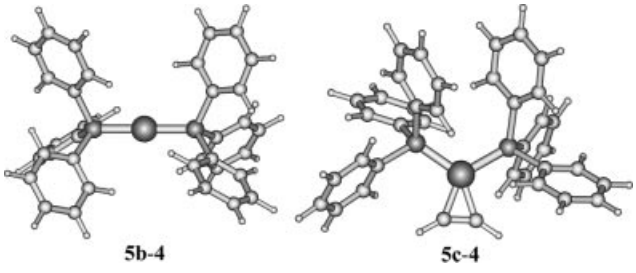

Figure 2. Optimized unsymmetrical molecular structures of **5b** and **5c**.

Table 1. Relative energies [kcal mol^{-1}] of the BP86/TZV(2df,2pd)-optimized rotamers of the metal fragments $Ni(PR_3)_2$ (**b**) and the acetylene complexes $C_2H_2Ni(PR_3)_2$ (**c**).

		R = H		R = CH_3		R = F		R = CF_3		R = C_6H_5	
Symm.	*n*	**1b-*n***	**1c-*n***	**2b-*n***	**2c-*n***	**3b-*n***	**3c-*n***	**4b-*n***	**4c-*n***	**5b-*n***	**5c-*n***
C_{2v}	1	0.1	0.0	0.0	0.0	0.1	0.1	0.0	0.0		
C_{2v}	2	0.0	0.2	0.0[a]	0.7	0.0	0.0	0.0[a]	0.9		
C_s	3	0.3	0.2	0.3	0.1	0.1	0.0[a]	0.0[a]	0.2	9.5	2.2
C_1	4									0.0	0.0

[a] Relative energies $\Delta E \leq 0.02$ kcal mol^{-1}.

Table 2. Selected optimized parameters of the most stable rotamers of the metal fragments $Ni(PR_3)_2$ (**b**), the acetylene complexes $C_2H_2Ni(PR_3)_2$ (**c**), and acetylene (**a**) in comparison with experimental data, where available.

R	Structure	Ni–P [Å]	Ni–C [Å]	C≡C [Å]	P–Ni–P (β) [°]	H–C–C (α) [°]
H	**1b-2**	2.084			148.4	
	1c-1	2.145	1.903	1.278	107.8	148.4
CH_3	**2b-1**	2.113			167.2	
	2c-1	2.161	1.879	1.286	114.8	145.2
F	**3b-2**	2.054			131.2	
	3c-2	2.094	1.914	1.269	108.1	152.5
CF_3	**4b-1**	2.080			144.7	
	4c-1	2.130	1.931	1.266	121.1	152.2
C_6H_5	**5b-4**	2.132			179.9	
	5c-4	2.185/2.189	1.902/1.911	1.279	115.6	148.5/149.2
	5c-4(exp)[a]	2.153/2.166	1.873/1.882	1.239		148.0
	C_2H_2			1.207		180.0
	C_2H_2(exp)			1.203		180.0

[a] X-ray data from ref.[6]

Table 3. Calculated energies [kcal mol^{-1}] for the reaction of acetylene (**a**) with $Ni(PR_3)_2$ (**b**) to give the complexes **c**, together with counterpoise corrected ΔE_3^{CP} and ΔE^{CP} values.[a]

R	Compl.	ΔE_1	ΔE_2	ΔE_3	ΔE	ΔE_3^{CP}	ΔE^{CP}
H	**1c-1**	+18.4	+13.1	–78.6	–47.1	–71.1	–39.6
CH_3	**2c-1**	+22.1	+16.8	–84.0	–45.1	–77.9	–39.0
CH_3[b]	**2c-1**	+22.5	+15.7	–126.3	–88.1	–108.8	–70.6
F	**3c-2**	+14.6	+7.6	–70.2	–48.0	–64.6	–42.4
CF_3	**4c-1**	+14.1	+8.3	–62.6	–40.2	–58.9	–36.5
C_6H_5	**5c-4**	+18.1	+16.9	–71.0	–36.0	–67.9	–32.9

[a] See Experimental Section for definition of the particular energy components. [b] Results obtained with the SV(d) basis set.

Table 4. Calculated occupancies of acetylene π, phosphorus lone-pair [Lp.(P)] and σ*(P–R) NBOs in complexes **1c**–**5c**.

		C_2H_2				PR_3	
R	Compl.	$\pi_\parallel$	$\pi_\perp$	$\pi_\parallel$*	$\pi_\perp$*	Lp.(P)	σ*(P–R)
H	**1c-1**	1.838	1.965	0.509	0.032	1.694	0.244
CH_3	**2c-1**	1.840	1.967	0.587	0.037	1.576	0.322
F	**3c-2**	1.836	1.956	0.456	0.024	1.505	0.653
CF_3	**4c-1**	1.826	1.957	0.418	0.026	1.617	0.682
C_6H_5	**5c-4**	1.842	1.963	0.520	0.039	1.581	0.380

crystallography.[6] Although the optimized bond lengths of **5c-4** are slightly longer than the experimental values (Table 2) the differences are not large (0.03–0.04 Å), and the most important geometrical features are well reproduced by the calculations. Taking into account that the theoretical data refer to the gas phase and are not subject to crystal-packing forces, such small deviations are understandable and are not considered relevant. Furthermore, it is well known that the BP86 functional usually slightly overestimates the bond lengths. The optimized bond lengths and angles of **1c-1** and **2c-1** are in good agreement with results obtained at different levels of theory in previous calculations.[2e,2i,2l]

The Ni–P bonds of **3c-2** (2.094 Å) and **4c-1** (2.130 Å) are shorter than those of **1c-1** (2.145 Å), **2c-1** (2.161 Å), and **5c-4** (2.185/2.189 Å). An opposite effect is observed for the nickel–acetylene bonds, where for complexes with electron-withdrawing substituents in the phosphane ligands the Ni–C bonds are longer [1.914 (**3c-2**) and 1.931 Å (**4c-1**)] than in the other investigated compounds (1.897–1.903 Å). The shortening of the Ni–P bonds as well as the lengthening of the Ni–C bonds of **3c-2** and **4c-1** vs. **1c-1**, **2c-1**, and **5c-4** can be well understood in the framework of the DCD model. The calculated occupancy of the σ*(P–R) NBOs of **3c-2** (0.653) and **4c-1** (0.682) is significantly higher than in the remaining compounds (0.244–0.380; Table 4). Thus, with respect to **1c-1**, **2c-1**, and **5c-4**, the Ni–σ*(P–R) back-bonding interactions of **3c-2** and **4c-1** are stronger. It is clear that an enhancement of Ni–σ*(P–R) backbonding shortens the Ni–P bonds and diminishes the competitive Ni–acetylene backbonding, which, in turn, leads to longer Ni–C bonds. Indeed, the occupancy of acetylene π* NBOs of **3c-2** and **4c-1** is significantly lower than that of **1c-1**, **2c-1**, and **5c-4** (Table 4).

Our results are consistent with the experimental observation that π-acceptor phosphanes normally exhibit shorter TM–P bonds.[17] Furthermore, Table 2 shows that substitution of PH_3 by $P(CH_3)_3$ and PPh_3 results in an elongation of the Ni–P bonds. It is interesting to note that similar properties have been observed in theoretical studies of $[Fe(CO)_4PR_3]$ compounds.[2f]

The coordination of acetylene (**a**) with $Ni(PR_3)_2$ (**b**) results in molecular deformations, which are obviously endothermic processes (Scheme 4, Table 3). Independent of the phosphane ligands, the deformation of acetylene (ΔE_1) requires more energy than that of the metal fragments $Ni(PR_3)_2$ (ΔE_2) (Table 3).

In complexes **c** acetylene is no longer linear and adopts a *cis* bent structure **d** with a significantly elongated C≡C bond (Table 2). The reasons for the deviation from linearity of coordinated alkynes are similar to those for the pyramidalization of complexed alkenes and have been discussed in detail in the literature.[14a,14b,18] Since, according to NBO population analyses, the electron-density distributions in acetylene with a deformed geometry **d** are the same as for the equilibrium geometry **a**, one can ask whether the deformation energy, ΔE_1, as well as the geometrical changes of the HC≡C bond angle, $\Delta\alpha$, and the C≡C bond length, $\Delta R_{C\equiv C}$, are influenced by the chemical nature of the phosphane ligands. In Figure 3 we present the deformation energies, ΔE_1, as a function of $\Delta\alpha$ and $\Delta R_{C\equiv C}$. From this figure it is evident that almost perfect linear correlations are found.

The ΔE_1 values increase in the order: $P(CF_3)_3 \geq PF_3 >> PPh_3 \geq PH_3 >> P(CH_3)_3$. Thus, phosphanes with electron-withdrawing substituents cause the smallest deformation of the acetylene ligand. Furthermore, the above ordering of the phosphane ligands essentially agrees with the predicted decrease of π-backbonding and an increase of σ-bonding contributions to the Fe–PR_3 bonds.[2f] It should also be noted that the inductive effects from the PH_3 and PPh_3 ligands on acetylene deformation are very similar, as re-

Table 5. Change of NBO occupancies in **1c**–**5c** relative to those of acetylene (**d**) and the corresponding molecular fragments **1e**–**5e**.[a]

R	Compl.	$\pi_\parallel$	$\pi_\perp$	$\pi_\parallel$*	$\pi_\perp$*	3s+3d$_\sigma$[b]	3d$_\pi$[b]	3d$_\delta$[b]	Lp	σ*(P–R)
H	**1c-1**	–0.16	–0.04	+0.51	+0.03	+0.14	–0.33	+0.01	–0.16	–0.04
CH_3	**2c-1**	–0.16	–0.03	+0.58	+0.04	+0.09	–0.34	+0.01	–0.12	–0.04
F	**3c-2**	–0.16	–0.04	+0.46	+0.02	+0.16	–0.27	+0.02	–0.14	–0.06
CF_3	**4c-1**	–0.17	–0.04	+0.42	+0.03	+0.12	–0.24	+0.02	–0.10	–0.02
C_6H_5	**5c-4**	–0.16	–0.04	+0.52	+0.04	+0.09	–0.30	+0.02	–0.06	–0.03

[a] Positive sign means an increase of NBO population due to complexation. [b] For the placement of the acetylene, nickel, and phosphorus atoms in the *yz*-plane, d$_\sigma$, d$_\pi$, and d$_\delta$ mean the d$_{z^2}$ d$_{yz}$, and d$_{xy}$ NBOs, respectively.

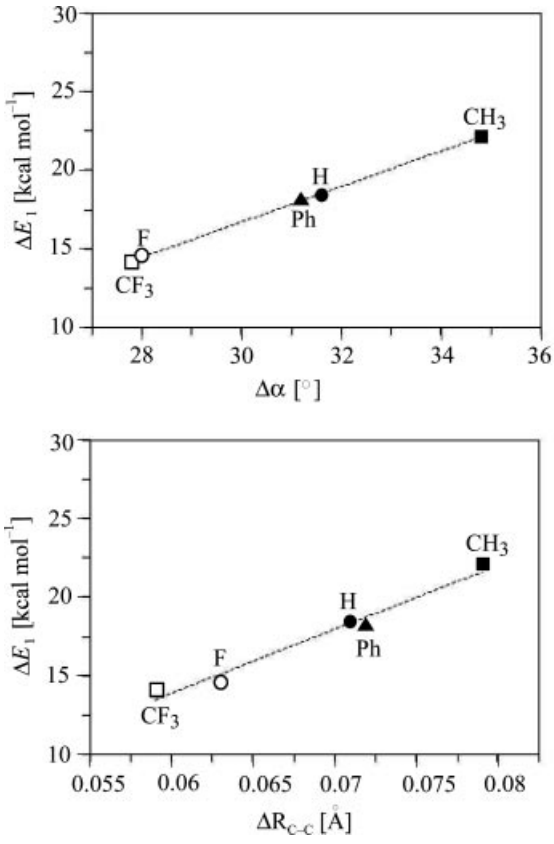

Figure 3. Deformation energy of acetylene (ΔE_1) as a function of the changes in the HC≡C bond angle $\Delta\alpha$ (top) and the C≡C bond length $\Delta R_{C\equiv C}$ (bottom) for the transformation from the equilibrium geometry **a** to the geometries **d** of the $[C_2H_2Ni(PR_3)_2]$ complexes **c** (R = H, CH_3, F, CF_3, and Ph).

flected by the very close ΔE_1, $\Delta\alpha$, and $\Delta R_{C\equiv C}$ values (Figure 3).

The optimized structures of the metal fragments **1b**–**4b** are bent, where the P–Ni–P bond angles, β, range from 131° to 167°, while **5b** prefers a linear arrangement of the P–Ni–P unit (Table 2, Figure 2). Our bent structures of **1b**–**4b** agree well with those obtained in an all-electron B3LYP study,[19] but are in disagreement with previous BP86/TZV and B3LYP/LANL2DZ calculations, where linear arrangements were found for the equilibrium geometries of **1b** and **2b**.[2e,2l] Nevertheless, the deformation energies, ΔE_2, of **1b-2** (+13.1 kcal mol^{-1}) and **2b-1** (+16.8 kcal mol^{-1}) are very close to those reported for the linear structures (12.7 and 16.4 kcal mol^{-1}, respectively).[2l] This suggests that the energies of **1b-2** and **2b-1** with a linear P–Ni–P unit should be close to those of the global-minimum bent structures with β angles of 148.4° and 167.2°, respectively (Table 2).

In Figure 4 we show the correlation between the deformation energies, ΔE_2, and the $\Delta\beta$ values for the transformation of the $Ni(PR_3)_2$ equilibrium structures **b** into geometries **e**, i.e., to those that they adopt in the corresponding complexes **c** (Scheme 4). Although the $Ni(PPh_3)_2$ fragment bends more strongly upon coordination with acetylene than the $Ni[P(CH_3)_3]_2$ one, the deformation energies, ΔE_2, are the same for both molecular units. This can be attributed to the fact that the distortion from the equilibrium structures **b** to geometries **e** leads not only to geometrical changes but also to different electron-density distributions. For the same reasons, no correlation was found between the ΔE_2 values and the changes in the Ni–P bond lengths. Similar to the ΔE_1 values of acetylene, the lowest ΔE_2 values are obtained for metal fragments with electron-withdrawing substituents (F and CF_3).

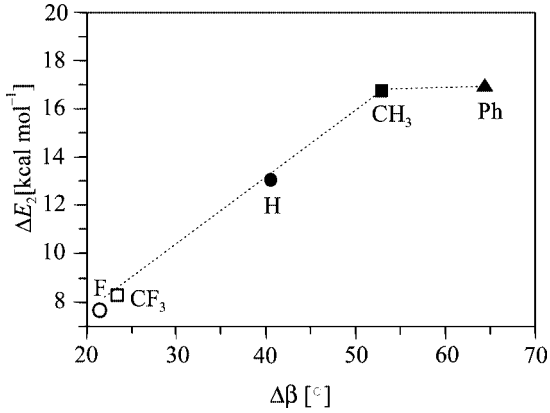

Figure 4. Deformation energy, ΔE_2, as a function of the change in the P–Ni–P bond angle, $\Delta\beta$, for the transformation of the $Ni(PR_3)_2$ (R = H, CH_3, F, CF_3, Ph) metal fragments from the equilibrium geometries **b** to complex geometries **e**.

Despite using large and flexible basis sets in our studies, the intrinsic interaction energies, ΔE_3, suffer from significant BSSE (Table 3). The BSSE contamination differs from one complex to the other. Thus, in the case of **3c-2** and **5c-4**, for example, the counterpoise corrections increase the difference of the bond-formation energies [$\Delta\Delta E_3 = \Delta E_3$(**3c-2**) – ΔE_3(**5c-4**)] from 0.8 to 3.3 kcal mol^{-1}, while an opposite effect is observed for **5c-4** and **1c-1**. The $\Delta\Delta E_3$ values of **5c-4** and **1c-1** diminish from 7.6 to 3.2 kcal mol^{-1} due to counterpoise corrections. Since relative energies are important for our discussion, in the following we will only consider the counterpoise corrected interaction energies. (Note that in theoretical investigations on TM compounds BSSE corrections are rather rarely taken into account, and when low-quality basis sets are used this may lead to wrong conclusions.) As an example, we recalculated the bond-formation process of **2c-1** by using the SV(d) basis set (Table 3). Although the use of the SV(d) basis set does not significantly change the distortion energies ΔE_1 and ΔE_2, the intrinsic interaction energy ΔE_3 (–126.3 kcal mol^{-1}) is largely overestimated as compared with the TZV(2df,2pd) value (–84.0 kcal mol^{-1}) and the BSSE contamination increases from 7.2% [TZV(2df,2pd)] to 13.9% [SV(d)] (Table 3).

In accord with the DCD model from Scheme 1, the bond-formation processes between acetylene (**d**) and the metal fragments $Ni(PR_3)_2$ (**e**) are accompanied by donor–acceptor interactions between both molecular fragments (Table 5).

The data from Table 5 confirm the very weak nature of the acetylene–nickel out-of-plane π-donation and δ-back-

donation interactions. The change in occupancy of acetylene $\pi_\perp$ and $\pi_\perp$* NBOs is much smaller than that of the $\pi_\parallel$ and $\pi_\parallel$* NBOs. In complexes **1c**–**5c**, the decrease of the occupancy of the acetylene $\pi_\parallel$ NBO is of the same magnitude and, consequently, the acetylene–nickel σ-donation interaction cannot be responsible for the different bond strengths. However, sufficiently large differences in NBOs' occupancies are discernible for acetylene–nickel π-backbonding interactions (Table 5). The increase of the occupancy of the acetylene $\pi_\parallel$* NBO as well as the decrease of the occupancy of the relevant Ni 3d$_\pi$ level shows a linear correlation with the intrinsic interaction energies, ΔE_3^{CP} (Figure 5). It should also be noted that analogous correlations of the entire interaction energies, ΔE^{CP}, are not found.

The changes of bond lengths during bond-formation or bond-breaking processes are often correlated with the bond strengths, i.e., with the corresponding ΔE or, more rigorously, ΔE^{CP} values. From the bottom of Figure 6, it is evident that such correlations do not exist either for the newly formed Ni–C bonds or for the elongation of the acetylene triple bond. However, a linear relationship is found with the intrinsic interaction energies ΔE_3^{CP} (Figure 6, top) for which the ordering of the PR_3 ligands [$P(CF_3)_3 < PF_3 < PPh_3 < PH_3 < P(CH_3)_3$] is the same as found for acetylene deformation energies ΔE_1 (Figure 3) or acetylene–nickel in-plane π-backbonding (Figure 5).

In agreement with the opinion of other authors,[2l] these findings point to the conclusion that the intrinsic interaction energies provide a better insight into the chemical nature of the ligand–metal bonds than the usually used ΔE (ΔE^{CP}) or D_e values. We are aware that the DCD model represents a simplified picture of the acetylene bonding as well as that the intrinsic interaction energies may be further decomposed into contributions from Pauli repulsion and electrostatic and orbital interaction terms. Nonetheless, the correlations from Figures 5 and 6 support the DCD bonding model for the nickel compounds investigated here.

The thermodynamics of bond-formation or bond-breaking processes depend upon the total interaction energies (ΔE^{CP} or D_e). In the case of the PH_3 and PPh_3 ligands the ΔE^{CP} values for acetylene bonding differ by 6.7 kcal mol^{-1} and therefore PH_3 cannot be considered as a good model for PPh_3. It is evident from Table 3 that this difference stems from the deformation energies, ΔE_2, of the $Ni(PH_3)_2$ and $Ni(PPh_3)_2$ fragments and the corresponding intrinsic interaction energies, ΔE_3^{CP}. Upon going from **5c-4** to **1c-1** the deformation energy, ΔE_2, decreases by 3.8 kcal mol^{-1}, the intrinsic interaction energy ΔE_3^{CP} increases by 3.2 kcal mol^{-1}, and the deformation energy of acetylene, ΔE_1, changes by only –0.3 kcal mol^{-1} (Table 3). On the other hand, similar ΔE^{CP} values to those of **1c-1** and **2c-1** do not necessarily indicate a very similar chemical nature of the acetylene bonding. **1c-1** and **2c-1** have almost the same ΔE^{CP} values (–39.6 and –39.0 kcal mol^{-1}, respectively), but their ΔE_3^{CP} values differ by 6.8 kcal mol^{-1} (Table 3). Finally, it should be noticed that the influence of phosphanes on the bonding properties of other ligands is not necessarily the same as in cases involving cleavage or formation of TM–P bonds. Thus, for example, the ΔE^{CP} values calculated for the cleavage of the Fe–PH_3 and Fe–$P(CH_3)_3$ bonds differ by about 10 kcal mol^{-1}, but with respect to PPh_3 the Fe–PH_3 bond is only 0.5 kcal mol^{-1} stronger.[2f] Since the computational advantage of using H instead of Ph is clear, one can ask whether the change of the cone angle of PH_3 may lead to a better model for PPh_3. Unfortunately, such changes affect the electronic structure and all energy components. Test calculations on **1c-1** with various cone angles of the PH_3 ligands have shown that it is not possible to predict whether and which contributions add up or cancel out without computational knowledge about the PPh_3 compound. Therefore, computational model systems should rather be avoided. In our case, calculations on the PH_3 com-

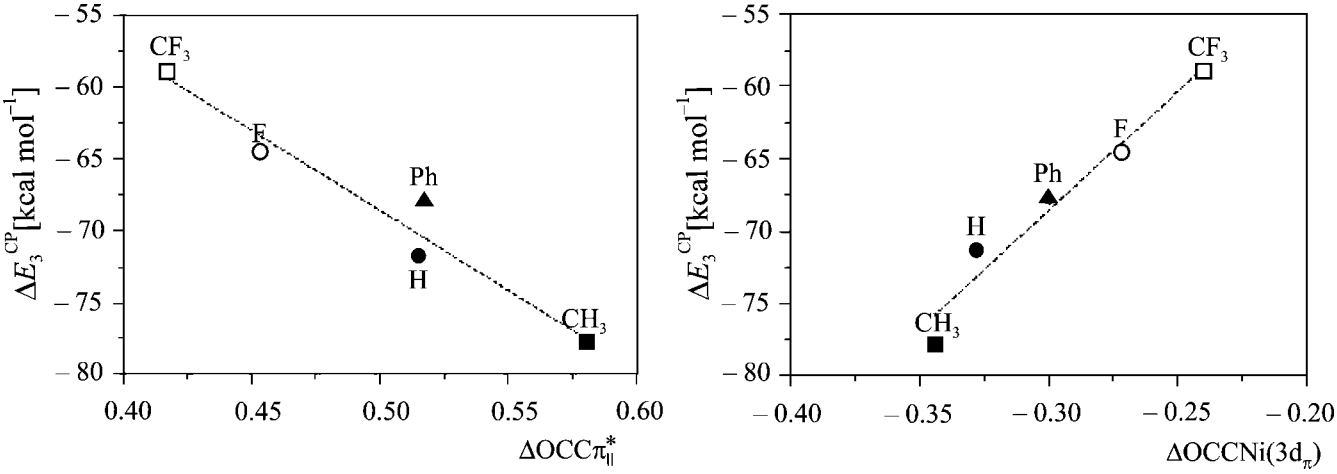

Figure 5. Correlation between intrinsic interaction energies, ΔE_3^{CP}, and changes of the occupancy of acetylene $\pi_\parallel$* NBO and the Ni 3d$_\pi$ level in complexes **1c**–**5c** relative to C_2H_2 (**d**) and the metal fragments $Ni(PR_3)_2$ (**e**) (R = H, CH_3, F, CF_3, Ph).

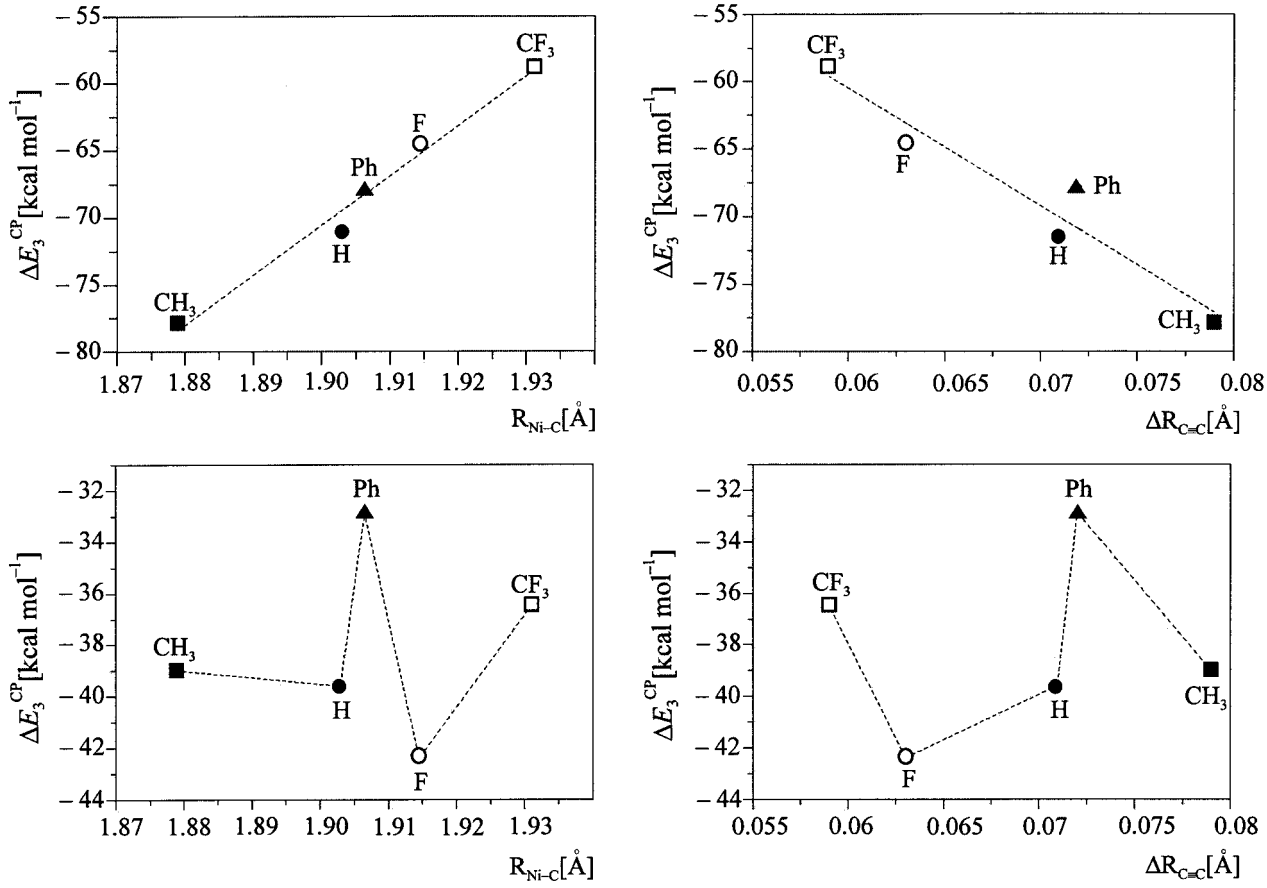

Figure 6. Correlation of the Ni–C bond lengths and the elongation of the C≡C bonds with the interaction energies ΔE_3^{CP} (top) and ΔE^{CP} (bottom) for the complexes $(C_2H_2)Ni(PR_3)_2$ (**c**) (R = H, CH_3, F, CF_3, Ph).

pound **1c-1** with the cone angles of PPh_3 from **5c-4** did not improve the model character of the PH_3 substitute.

Concluding Remarks

In this study we have investigated the structures and energetics for the bond-formation processes between acetylene and the metal fragments $Ni(PR_3)_2$. We were interested in the question of how the substituents R (H, CH_3, F, CF_3 and Ph) in the phosphane ligands influence the nickel–acetylene bonding as well as whether the PPh_3 ligand may be modeled in computational studies by smaller, i.e., computationally less demanding, phosphanes. The bond-formation processes were analyzed in terms of distortion energies of acetylene (ΔE_1) and $Ni(PR_3)_2$ (ΔE_2), intrinsic interaction energies (ΔE_3), and the DCD model. We have shown that despite using large TZV(2df,2pd) basis sets, BSSE still contaminates the ΔE_3 values by 5–10% and therefore should be considered in accurate studies, especially in cases where double-ς basis sets with only a single polarization function are used. The effects of phosphane substituents on nickel–acetylene bonding cannot be correlated with total interaction energies (ΔE^{CP} or D_e), although linear correlations were found between the intrinsic interaction energies ΔE_3^{CP} and (i) the acetylene–nickel in-plane π-backbonding interactions, (ii) the distances of the newly formed Ni–C bonds, and (iii) the elongation of the acetylene triple bond. In these correlations the ΔE_3^{CP} values change in the order $P(CF_3)_3 < PF_3 < PPh_3 < PH_3 < P(CH_3)_3$. The total interaction energies increase in the order $PPh_3 < P(CF_3)_3 < P(CH_3)_3 < PH_3 < PF_3$. The effects of the phosphane ligands PPh_3 and PH_3 on the thermodynamics of acetylene bonding are different and therefore PH_3 cannot be regarded as a good substitute of PPh_3. The differences stem in an almost equal footing from the deformation energies of the metal fragments (ΔE_2) and the intrinsic interaction energies (ΔE_3^{CP}).

Experimental Section

Calculational Details: The geometry optimizations of the complexes $C_2H_2Ni(PR_3)_2$ (**c**) and their molecular fragments C_2H_2 (**a**) and $Ni(PR_3)_2$ (**b**) were carried out with the TURBOMOLE 5.6 suite of programs.[20] As a quantum chemical method we have used density functional theory (DFT)[21] with the gradient-corrected BP86 functional[22] and the RI approximation which takes advantage of density fitting for the calculations of the Coulomb integrals.[23] All atoms were described with an all-electron valence triple-ς basis set augmented with polarization functions: (17s11p6d1f)/[6s4p3d1f] for Ni, (14s9p2d1f)/[5s5p2d1f] for P, (11s6p2df)/[5s3p2df] for C and F, and (6s2pd)/[3s2pd] for H, which we denote as TZV(2df,2pd). These basis sets, together with the corresponding auxiliary basis

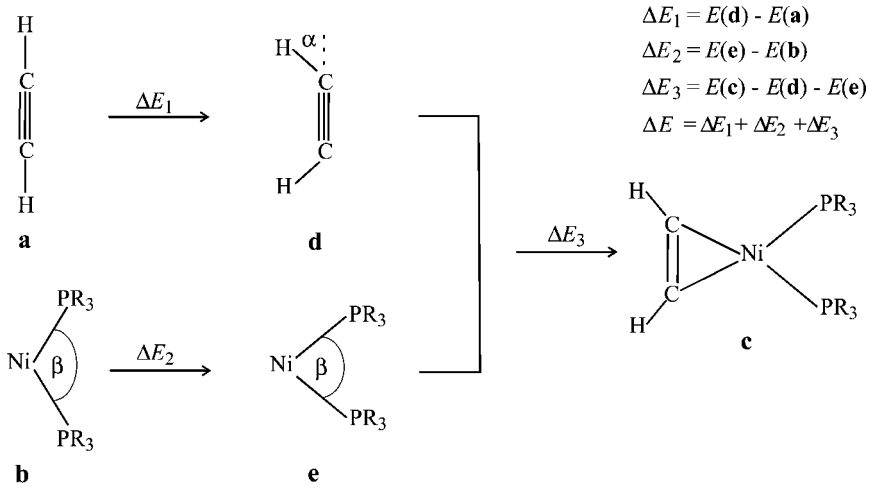

Scheme 4.

sets for the RI approximation, were taken from the TURBOMOLE basis set library.[24] Note that the TZV(2df,2pd) basis sets used here are of significantly higher quality than those employed in many previous theoretical studies on TM compounds of similar size.

The nature of ligand–metal bonds is usually discussed in terms of bond dissociation energies, D_e. It is obvious that the bond-formation energy of acetylene (**a**) with fragments $Ni(PR_3)_2$ (**b**) to give the complexes **c**, ΔE, is equal to the negative of the dissociation energy D_e, see Equation (1).

$$-D_e = \Delta E = E(\mathbf{c}) - [E(\mathbf{a}) + E(\mathbf{b})] \quad (1)$$

$E(\mathbf{c})$, $E(\mathbf{a})$, and $E(\mathbf{b})$ are the total energies of the corresponding equilibrium structures. In order to obtain deeper insight into acetylene–nickel bonding, the bond-formation energy, ΔE, was partitioned into deformation (also called preparation) energies (ΔE_1 and ΔE_2) and the intrinsic interaction energy (ΔE_3), as shown in Scheme 4.

ΔE_1 and ΔE_2 are the energies that are necessary to transform acetylene (**a**) and $Ni(PR_3)_2$ (**b**) from their equilibrium geometries into the geometries that they adopt in the complexes **c**. ΔE_3 represents the intrinsic interaction energy between the two "prepared" fragments **d** and **e** in the complex **c**. This partitioning scheme allows us to correct the intrinsic interaction energy (ΔE_3) and, consequently, the bond-formation energy, ΔE, for basis set superposition error (BSSE). The BSSE was calculated according to the counterpoise method[25] and the corrected energies are denoted as ΔE_3^{CP} and ΔE^{CP}. The bond-formation processes were calculated for the closed-shell singlet states of the complexes **c** and their molecular fragments **a**,**d** and **b**,**e**. The electron-density distributions in complexes **c** and the molecular fragments **a**,**d** and **b**,**e** were investigated with the help of natural bond orbital (NBO) procedures.[26] Calculations of the harmonic frequencies for the equilibrium structures were carried out with the SNF program.[27]

Acknowledgments

This work was supported by the Deutsche Forschungsgemeinschaft in the framework of the SFB 424 ("Molekulare Orientierung als Funktionskriterium in chemischen Systemen").

[1] a) F. R. Hartley, *Comprehensive Organometallic Chemistry* (Ed.: G. Wilkinson), Pergamon Press: Oxford, **1982**; b) P. W. Jolly, G. Wilke, *The Organic Chemistry of Nickel*, Academic Press, New York, **1975**; c) W. Reppe, *Neue Entwicklungen auf dem Gebiet des Acetylens und Kohlenmonooxids*, Springer-Verag, Berlin, **1979**.

[2] a) T. A. Albright, R. Hoffmann, J. C. Thibault, D. L. Thorn, *J. Am. Chem. Soc.* **1979**, *101*, 3801–3812; b) K. Kitaura, S. Sakaki, K. Morokuma, *Inorg. Chem.* **1981**, *20*, 2292–2297; c) T. Ziegler, *Inorg. Chem.* **1985**, *24*, 1547–1552; d) Z. Lin, M. B. Hall, *J. Am. Chem. Soc.* **1992**, *114*, 2928–2932; e) J. Li, G. Schreckenbach, T. Ziegler, *Inorg. Chem.* **1995**, *34*, 3245–3252; f) Ò. González-Blanco, V. Branchadell, *Organometallics* **1997**, *16*, 5556–5562; g) H. Jacobsen, H. Berke, *Chem. Eur. J.* **1997**, *3*, 881–886; h) R. Schmid, W. A. Herrmann, G. Frenking, *Organometallics* **1997**, *16*, 701–708; i) I. Hyla-Kryspin, J. Koch, R. Gleiter, T. Klettke, D. Walther, *Organometallics* **1998**, *17*, 4724–4733; j) F. Nunzi, A. Sgamellotti, N. Re, C. Floriani, *Dalton. Trans.* **1999**, 3487–3491; k) G. Frenking, N. Fröhlich, *Chem. Rev.* **2000**, *100*, 717–774; l) C. Massera, G. Frenking, *Organometallics* **2003**, *22*, 2758–2765.

[3] a) G. Wilke, *Angew. Chem.* **1957**, *69*, 397–398; b) G. Wilke, G. Herrmann, *Angew. Chem.* **1962**, *74*, 693–694; *Angew. Chem. Int. Ed. Engl.* **1962**, *1*, 549–550; c) E. J. Corey, M. F. Semmelhack, *J. Am. Chem. Soc.* **1967**, *89*, 2755–2757; d) G. Wilke, *Pure Appl. Chem.* **1968**, *17*, 179–194; e) P. W. Jolly, I. Tkatchenko, G. Wilke, *Angew. Chem.* **1971**, *83*, 328–329; *Angew. Chem. Int. Ed. Engl.* **1971**, *10*, 328–329; f) M. F. Semmelhack, P. M. Helquist, L. D. Jones, *J. Am. Chem. Soc.* **1971**, *93*, 5908–5910; g) M. F. Semmelhack, *Org. React.* **1972**, *19*, 115–198; h) M. F. Semmelhack, P. M. Helquist, J. D. Gorzynski, *J. Am. Chem. Soc.* **1972**, *94*, 9234–9236; i) G. Wilke, *Angew. Chem.* **1988**, *100*, 189–211; *Angew. Chem. Int. Ed. Engl.* **1988**, *27*, 185–207 and references cited therein.

[4] See also: a) M. Torrent, M. Solà, G. Frenking, *Chem. Rev.* **2000**, *100*, 439–493 and references cited therein; b) W. Siebert, G. Wilke, *J. Organomet. Chem.* **2002**, *641*, 1–2.

[5] a) W. Reppe, W. Sweckendiek, *Justus Liebigs Ann. Chem.* **1948**, *560*, 104–116; b) W. Reppe, O. Schlichting, H. Meister, *Justus Liebigs Ann. Chem.* **1948**, *560*, 93–104; c) W. Reppe, O. Schlichting, K. Klager, T. Toepel, *Justus Liebigs. Ann. Chem.* **1948**, *560*, 1–92.

[6] K. R. Pörschke, Y.-H. Tsay, C. Krüger, *Angew. Chem.* **1985**, *97*, 334–335; *Angew. Chem. Int. Ed. Engl.* **1985**, *24*, 323–324.

[7] C. A. Tolman, *J. Am. Chem. Soc.* **1970**, *92*, 2953–2956.

[8] a) K. R. Pörschke, R. Mynott, K. Angermund, C. Krüger, *Z. Naturforsch., Teil B* **1985**, *40*, 199–209; b) U. Rosenthal, G. Oehme, H. Görls, V. V. Burlakov, A. V. Polyakov, A. I. Yanovsky, Yu. T. Struchkov, *J. Organomet. Chem.* **1990**, *389*, 409–416: c) U. Rosenthal, G. Oehme, H. Görls, V. V. Burlakov, A. V. Polyakov, A. I. Yanovsky, Yu. T. Struchkov, *J. Organomet. Chem.* **1990**, *390*, 113–120; d) T. Bartic, B. Happ, M. Iglewsky, H. Bandmann, R. Boese, P. Heimbach, T. Hoffmann, E. Wenschuh, *Organometallics* **1992**, *11*, 1235–1241: e) U. Rosenthal, C. Nauck, P. Arndt, S. Pulst, W. Baumann, V. V. Burlakov, H. Görls, *J. Organomet. Chem.* **1994**, *484*, 81–87.

[9] a) M. J. S. Dewar, *Bull. Soc. Chim. Fr.* **1951**, C71–C79; b) J. Chatt, L. A. Duncanson, *J. Chem. Soc.* **1953**, 2939–2947.

[10] a) S.-X. Xiao, W. C. Trogler, D. E. Ellis, Z. Berkovitch-Yellin, *J. Am. Chem. Soc.* **1983**, *105*, 7033–7037; b) J. A. Tosell, J. H. Moore, J. C. Giordan, *Inorg. Chem.* **1985**, *24*, 1100–1103; c) B. J. Dunne, R. B. Morris, A. G. Orpen, *J. Chem. Soc. Dalton Trans.* **1991**, 653–661.

[11] a) P. B. Dias, M. E. Minas de Piedade, J. A. Martinho Simões, *Coord. Chem. Rev.* **1994**, *135/136*, 737–807: b) R. S. Drago, *Organometallics* **1995**, *14*, 3408–3417; c) S. P. Wang, M. G. Richmond, M. Schwarz, *J. Am. Chem. Soc.* **1992**, *114*, 7595–7596; d) J. Bartholomew, A. L. Fernandez, B. A. Lorsbach, M. R. Wilson, W. P. Giering, *Organometallics* **1996**, *15*, 295–301.

[12] a) D. S. Marynick, *J. Am. Chem. Soc.* **1984**, *106*, 4064–4065; b) M. R. A. Blomberg, U. B. Brandemark, P. E. M. Siegbahn, K. B. Mathisen, G. Karlström, *J. Phys. Chem.* **1985**, *89*, 2171–2180; c) T. L. Brown, *Inorg. Chem.* **1992**, *31*, 1286–1294; d) G. Pacchioni, P. S. Bagus, *Inorg. Chem.* **1992**, *31*, 4391–4398; e) M.-G. Choi, T. L. Brown, *Inorg. Chem.* **1993**, *32*, 5603–5610; f) O. D. Häberlen, N. Rösch, *J. Phys. Chem.* **1993**, *97*, 4970–4973; g) P. Fantucci, S. Polezzo, M. Sironi, A. Bencini, *J. Chem. Soc. Dalton Trans.* **1995**, 4121–4126.

[13] a) O. S. Mills, B. W. Shaw, *J. Organomet. Chem.* **1968**, *11*, 595–699; b) Y. Wang, P. Coppens, *Inorg. Chem.* **1976**, *15*, 1122–1127; c) R. J. Restiva, G. Ferguson, T. W. Ng, A. Carty, *Inorg. Chem.* **1977**, *16*, 172–176; d) D. Walther, A. Schmidt, T. Klettke, W. Imhoff, H. Görls, *Angew. Chem.* **1994**, *106*; 1421–1424; *Angew. Chem. Int. Ed. Engl.* **1994**, *33*, 1373–1376; e) D. Walther, T. Klettke, H. Görls, *Angew. Chem.* **1995**, *107*, 2022–2023; *Angew. Chem. Int. Ed. Engl.* **1995**, *34*, 1860–1861; f) D. Walther, T. Klettke, A. Schmidt, *Organometallics* **1996**, *15*, 2314–2319.

[14] a) D. M. Hoffman, R. Hoffmann, *J. Chem. Soc. Dalton Trans.* **1982**, 1471–1482; b) D. M. Hoffman, R. Hoffmann, R. Fisel, *J. Am. Chem. Soc.* **1982**, *104*, 3858–3875; c) D. J. Underwood, M. Nowak, R. Hoffmann, *J. Am. Chem. Soc.* **1984**, *106*, 2837–2847; d) J. Koch, I. Hyla-Kryspin, R. Gleiter, T. Klettke, D. Walther, *Organometallics* **1999**, *18*, 4942–4948.

[15] S.-Q. Niu, M. B. Hall, *Chem. Rev.* **2000**, *100*, 353–405 and references cited therein.

[16] T. A. Albright, J. K. Burdett, M.-H. Whangbo, *Orbital Interactions in Chemistry*, Wiley, New York, **1985**.

[17] a) H.-Y. Liu, K. Eriks, A. Prock, W. P. Giering, *Organometallics* **1990**, *9*, 1758–1766; b) K. G. Moloy, J. L. Peterson, *J. Am. Chem. Soc.* **1995**, *117*, 7696–7710.

[18] K. Morokuma, W. T. Borden, *J. Am. Chem. Soc.* **1991**, *113*, 1912–1914.

[19] J. Koch, Dissertation: Der Mechanismus der Ni^0-katalysierten Hydrocyanierung von Ethen und Propen, Quantenchemische Modellrechnungen, University of Heidelberg, **1997**.

[20] a) R. Ahlrichs, M. Bär, H.-P. Baron, R. Bauernschmitt, S. Böcker, M. Ehrig, K. Eichkorn, S. Elliot, F. Furche, F. Haase, M. Häser, H. Horn, C. Huber, U. Huniar, M. Kattannek, C. Kölmel, M. Kollwitz, K. May, C. Ochsenfeld, H. Öhm, A. Schäfer, U. Schneider, O. Treutler, M. von Arnim, F. Weigend, P. Weis, H. Weiss, TURBOMOLE, Ver. 5.6; University of Karlsruhe, **2003**.; b) M. von Arnim, R. Ahlrichs, *J. Comput. Chem.* **1998**, *19*, 1746–1757.

[21] R. G. Parr, W. Yang, *Density-Functional Theory of Atoms and Molecules*, Oxford University Press, Oxford, **1989**.

[22] a) A. D. Becke, *Phys. Rev. A* **1988**, *38*, 3098–3100; b) J. P. Perdew, *Phys. Rev. B* **1986**, *33*, 8822–8824.

[23] a) K. Eichkorn, O. Treutler, H. Öhm, M. Häser, R. Ahlrichs, *Chem. Phys. Lett.* **1995**, *242*, 652–660; b) O. Treutler, R. Ahlrichs, *J. Chem. Phys.* **1995**, *102*, 346–354.

[24] The basis sets are available from the TURBOMOLE homepage http://www.turbomole.com via the FTP Server Button in the subdirectories basen and jbasen (auxiliary basis set for RIDFT calculations).

[25] S. F. Boys, F. Bernardi, *Mol. Phys.* **1970**, *19*, 553–566.

[26] a) J. P. Foster, F. Weinhold, *J. Am. Chem. Soc.* **1980**, *102*, 7211–7218; b) A. E. Reed, F. Weinhold, *J. Chem. Phys.* **1983**, *78*, 4066–4073; c) A. E. Reead, R. B. Weinstock, F. Weinhold, *Chem. Rev.* **1988**, *88*, 899–926; e) J. E. Carpenter, F. Weinhold, *J. Mol. Struct. (THEOCHEM)* **1988**, *169*, 41.

[27] C. Kind, M. Reiher, J. Neugebauer, B. Hess, SNF (Vers.2.2.1), A program for numerical frequency analyses, University of Erlangen, **2002**.

Received: July 25, 2005
Published Online: November 17, 2005

